Heliyon 9 (2023) e18828

Contents lists available at ScienceDirect

Heliyon

journal homepage: www.cell.com/heliyon

Research article

Nanowarming improves survival of vitrified ovarian tissue and follicular development in a sheep model

Sareh Karimi [a,d], Seyed Nasrollah Tabatabaei [b,c], Marefat Ghaffari Novin [a], Mahsa Kazemi [a], Zahra Shams Mofarahe [a,**], Alireza Ebrahimzadeh-Bideskan [d,e,*]

[a] Department of Biology and Anatomical Sciences, School of Medicine, Shahid Beheshti University of Medical Sciences, Tehran, Iran
[b] Department of Medical Nanotechnology, School of Advanced Technologies in Medicine, Tehran University of Medical Sciences, Tehran, Iran
[c] Department of Pediatrics, Physiology and Pharmacology, University of Montreal, Montreal, Qc, Canada
[d] Department of Anatomy and Cell Biology, School of Medicine, Mashhad University of Medical Sciences, Iran
[e] Applied Biomedical Research Center, Mashhad University of Medical Sciences, Mashhad, Iran

ARTICLE INFO

Keywords:
Ovary
Cryopreservation
Vitrification
Warming
Nanoparticle

ABSTRACT

Tissue cryopreservation has allowed long term banking of biomaterials in medicine. Ovarian tissue cryopreservation in particular helps patients by extending their fertility window. However, protection against tissue injury during the thawing process has proven to be challenging. This is mainly due to the heterogenous and slow distribution of the thermal energy across the vitrified tissue during a conventional warming process. Nanowarming is a technique that utilizes hyperthermia of magnetic nanoparticles to accelerate this process. Herein, hyperthermia of synthesized PEGylated silica-coated iron oxide nanoparticles was used to deter the injury of cryopreserved ovarian tissue in a sheep model. When compared to the conventional technique, our findings suggest that follicular development and gene expression in tissues warmed by the proposed technique have been improved. In addition, Nanowarming prevented cellular apoptosis and oxidative stress. We therefore conclude that Nanowarming is a potential complementary candidate to increase efficiency in the ovarian cryopreservation field.

1. Introduction

1.1. Background

Cancer, with an increasing prevalence in recent years, affects about 10% of the female population under the age of 45 [1]. Adopted strategies for treatment, such as radiotherapy and chemotherapy, are often associated with serious adverse side effects on healthy tissue, including the reproductive organs [2,3]. Depending on the patient's condition and her cancer stage, cryopreservation of embryos, oocytes, and ovarian tissue may be recommended [3].

Cryopreservation of the ovarian tissue is medically preferred for pre-pubertal girls, adolescents, single women, and generally

* Corresponding author. Department of Anatomy and Cell Biology, School of Medicine, Mashhad University of Medical Sciences, Azadi Sq., Vakilabad Blvd., P.O. Box 91779-48564, Mashhad, Iran.
** Corresponding author. Department of Biology and Anatomical Sciences, Faculty of Medicine, Shahid Beheshti University of Medical Sciences, Velenjak, Tehran, Iran.
E-mail addresses: z_shams@sbmu.ac.ir (Z.S. Mofarahe), ebrahimzadehBA@mums.ac.ir (A. Ebrahimzadeh-Bideskan).

https://doi.org/10.1016/j.heliyon.2023.e18828
Received 14 November 2022; Received in revised form 12 July 2023; Accepted 31 July 2023
Available online 8 August 2023

patients with limited time to undergo ovarian stimulatory cycles [2,3]. In this process, the functional part of the ovary known as the cortical layer is cryopreserved [4]. The first report of human ovarian tissue cryopreservation was in 2000 [5], whereas until 2017, 84 live births and 8 ongoing pregnancies have been reported and the live birth rate after ovarian tissue cryopreservation and autologous transplantation is more than 37% per women [6] and it is predicted that by the year 2020 more than 200 live birth occur following this technique [7]. However, cryopreservation faces certain challenges; although follicles, in the cortex of the ovaries that contain developing oocytes, are supported by the surrounding stromal cells [8], tissue injury during cryopreservation affects the outcome of the procedure by either decreasing the ovarian reserve, or disturbing the stromal tissue [9]. Tissue injury during cryopreservation may be occur in different steps, that in many researches try to solve them, for example use of cryoprotectants can induce cytotoxicity [10] and decline the tissue viability, that dose, combination, time and etc. of cryoprotectants are the challenges in some researches [11], and cryoinjury that results from both vitrification and the consequent warming of the sample. During these processes, spontaneous ice formation caused by a temperature shift between −5 °C and −15 °C [12] and non-uniform distribution of heat in the warming process [13] induces mechanical and oxidative stress on tissue and affects cellular functions [14]. Specifically, lipid peroxidation of cell membranes, assessed by the level of malondialdehyde (MDA), is an example of a cryoinjury-induced by oxidative stress [15]. Furthermore, mechano-chemical stress causes adverse effects on the expression of developmental genes [16]. Indeed, cryoinjury can alter the expression of growth differentiation factor-9 (GDF-9) as well as bone morphogenetic protein-15 (BMP15) that are involved in oocyte maturation and transition from primary to secondary follicles, respectively [17]. Furthermore, follicle-stimulating hormone receptor (FSHR) which is an indicator of follicle transition from secondary to antral state [18] can be affected by cryoinjury.

To minimize injuries, numerous attempts have been made to improve cryopreservation protocols. Among these, a vitrification technique with accelerated cooling rate, such as method described by Kagawa et al. [12,19,20], has shown extensive reduction in ice formation during vitrification process. The warming portion of the process however, demands improvement [21] due to lack of a uniform distribution of thermal energy in the preserved sample [22,23]. During warming, the surface of the tissue quickly reaches thermal equilibrium while temperature exchange in deeper layers occurs slowly. The resulting thermal gradient in the sample thereby leads to formation of ice crystals [24] and subsequent thermal stress.

To overcome these challenges, various volumetric heating techniques including application of radiofrequency [25,26] and microwave [27,28] have been suggested. However, generation of heat by electromagnetic radiation may result in heterogenous thermal distribution as heat conductivity varies throughout the sample [21]. To address this shortcoming, generation of heat by induction of magnetic nanoparticles has been proposed [24]. Briefly, magnetic nanoparticles can be remotely excited once placed inside an alternating magnetic field (AMF). A coil connected to an AMF generator produce AMF [29]. Every time the direction of the magnetic field changes, magnetic nanoparticles release their absorbed energy in the form of heat to their surroundings. This provides an accelerated and more uniform warming process known as Nanowarming [13,30], where it has been introduced to protect cryopreserved porcine aortic heart valve leaflet tissue [31]. Magnetic nanoparticles are is the main group of nanoparticles with biomedical applications for example in tissue engineering [32], drug delivery [33] and magnetic resonance imaging (MRI) contrast agent [34]. Iron oxide nanoparticle is one of the magnetic nanoparticles with more usage than other because it has high bio-compatibility and bio-distribution, moreover for some condition it was approved by the food and drug administration (FDA). The FDA permits the use of magnetic nanoparticles as contrast agents in MRI, cancer treatment and drug release as heat mediators by using AMF [35]. The mature sheep ovary is introduced as standard model for cryopreservation of human ovarian tissue because [36]it is similar to the human ovary in terms of dense stromal tissue and high density of follicles in cortex and the duration of follicular development is prolong as human, so sheep is the good model for follicle development studies after cryopreservation [37,38].

In this study, Nanowarming was performed by adding PEGylated silica-coated iron oxide nanoparticles to the vitrification media that was used to cryopreserve fragments of the ovarian cortex of a sheep model. To warm the cryopreserved tissues, the cryovials were placed inside an AMF for 1 min. The tissue fragments were then cultured for 8 days and compared to the conventional method for the ovarian tissue cryopreservation (see graphical abstract). Herein, the tissue injury of the proposed technique has been thoroughly assessed and compared with previous approaches.

2. Materials and methods

All procedures were performed in accordance with the guidelines approved by the Shahid Beheshti University of Medical Sciences Ethics Committee (IR.SBMU.MSP.REC.1398.981). This study was designed to evaluate the efficacy of coupling Nanowarming to a vitrification procedure described by Kagawa et al. [39].

Tissue divided into two main groups, cultured and non-cultured. In all groups, oxidative stress and gene expression were measured, follicles were counted (after H&E staining) to evaluate the folliculogenesisand the viability and function of tissue were assessed in cultured groups.

2.1. Ovarian tissue collection

Ovaries (N = 24) from sheep aged 1–2 years old, without a history of pregnancy were procured. The samples were taken from slaughtered animals (Mashhad, Iran) where no sheep was sacrificed for the sole purpose of this research. After dissection, the ovaries were immediately placed in a solution of Hams F10 (Biowest, France) supplemented with 50 mg/ml streptomycin, 60 IU/ml penicillin (Gibco, UK), 10% human serum albumin (HSA) (Daru Pakhsh, Iran), and kept at 4 °C. In the laboratory, the ovaries were washed three times with fresh sterile PBS and placed in sterile petri dishes that contained warm supplemented Hams F10 with HEPES (Biowest, France) buffer, 10% HSA, 50 mg/ml streptomycin, and 60 IU/ml penicillin. Next, the medulla of each ovary was discarded, and the

remaining cortex was sliced into approximate volumes of 1 mm^3 then pooled and randomly divided into: a) freshly dissected tissue (Fresh), b) conventional vitrification followed by warming (Convl-Vit), c) vitrification followed by Nanowarming (Nano-Vit), and d) vitrification followed by placement of the sample in an alternating magnetic field (AMF). Then, the dissected tissues in every group were randomly divided into two subgroups, one of which underwent cryopreservation and then culture (in 96-well culture plates) for 8 days (Cultured groups) [40] and another subgroup evaluated after cryopreservation (Non-Cultured groups) (see Fig. 1).

2.2. Synthesis of nanoparticles

PEGylated silica-coated superparamagnetic iron oxide nanoparticles (IONP@Si@PEG) were chemically synthesized via a method previously described in Refs. [41,42]. In brief, 2 g of $FeCl_3$ (Merck, Germany) was added and completely mixed to an equal amount of $FeSO_4$ (Sigma-Aldrich, USA) in 1-liter of ultra-distilled water at room temperature. The resulting solution was deoxygenated with perching of nitrogen into the reaction system [43] and then ammonium hydroxide was added. The precipitated particles were isolated by a magnet, washed with ethanol, and kept under oxygen-free conditions. Then, the particles were dispersed in deionized water and coated with silica by adding Tetraethyl orthosilicate (TEOS) (Merck, Germany). Finally, the particles were PEGylated in a PEG-silane (Merck, Germany) solution. After synthesis, the resulting IONP@Si@PEG were characterized with Dynamic Light Scattering (DLS), Zeta-potential (SZ-100 Nanoparticle Analyzer – Horiba, Japan), X-Ray Diffraction (XRD) (Philips PW 1730, Germany), Fourier Transform Infrared Spectroscopy (FTIR) (Thermo Nicolet AVATAR 370 FTIR) and Transmission Electron Microscopy (TEM) (Leo 912 Ab Omega, Zeiss) operated at 120 kV and the toxicity of IONP@Si@PEG evaluated in our pervious study [44].

2.3. Vitrification, warming and nanowarming

2.3.1. Vitrification

In this study, a vitrification method introduced by Kagawa [20] was applied with some modification. Briefly, the ovarian cortical fragments were washed three times with HamsF10, then they were immersed in equilibration solution (ES) containing HamsF10 supplemented with 20% HSA, 7.5% ethylene glycol (EG) (Merck, Germany), and 7.5% dimethyl sulphoxide (DMSO) (Merck, Germany) for 25 min in room temperature. Then, the fragments were dried with filter paper and immersed in vitrification solution (VS) containing HamsF10 supplemented with 10% HSA and 20% EG, 20% DMSO, and 0.5 mol/l sucrose for 15 min in room temperature. Finally, the fragments were transferred to cryovials with 100 μl VS, were kept on nitrogen vapor for 30 s, and then stored in the liquid nitrogen for approximately one week [45,46].

2.3.2. Warming

In the warming process, the cryovials were recovered and placed in a 37 °C water bath for the VS to completely defrost. Then, fragments were immediately transferred to first warming solution containing HamsF10 supplemented with 20% HSA and 1 mol/L sucrose (Merck, Germany) at 37 °C for 3 min. Next, the fragments were placed in a second warming solution containing HamsF10 supplemented with 20% HSA and 0.5 mol/L sucrose for 5 min. Finally, the fragments were immersed in HamsF10 supplemented with 20% HSA for 3 min prior to any assessments being made (the group under this process is conventional vitrification and warming (Convl-Vit).

2.3.3. Nanowarming

Prior to vitrification, IONP@Si@PEG were added to the VS at a concentration of 10 mg Fe/ml [31] and the vitrification protocol was carried out as described in 2-3-1. For the subsequent tissue warming, the vitrified fragments in cryovials were immediately placed at the center of a hollow copper coil with 5 cm in diameter and 8 cm in length. The coil was connected to an AMF generator (MSI Automation, USA) exposing the sample to a field strength of 26 kA/m at 400 kHz for 1 min. Then, the warming procedure was

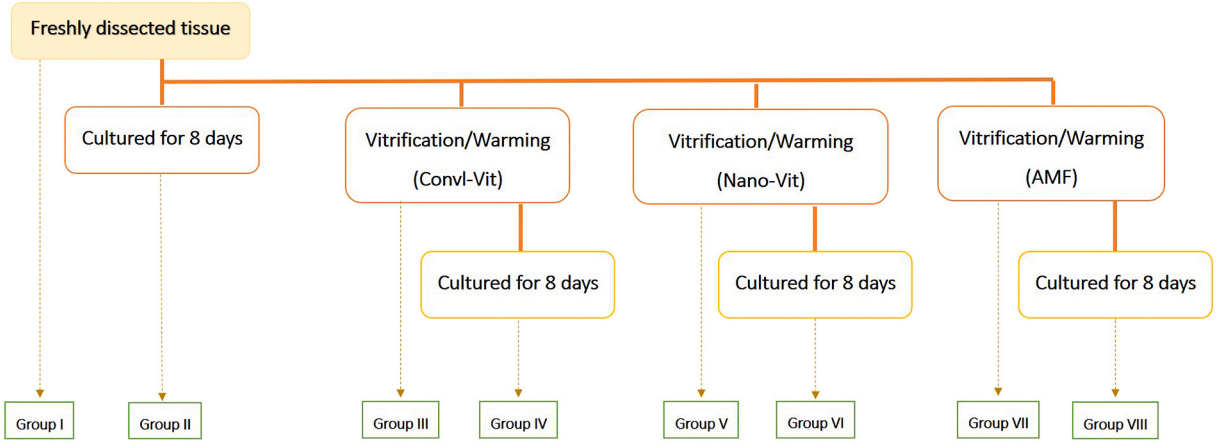

Fig. 1. Experimental design. This schematic illustrates the treatments applied to groups I through VIII. Each group consists of 26 fragments.

performed as described in 2-3-2 (the group under this process is vitrification with nanowarming (Nano-Vit).

2.3.4. Warming in AMF

To evaluate the effect of magnetic field alone on the warming process, the cryovials containing vitrified tissue fragments without IONP@Si@PEG were placed inside a hollow copper coil as described in the previous section for 1 min. Then, the warming process similar to 2-3-2 was followed (the group under this process is vitrification and warming in alternative magnetic field (AMF).

2.4. Ovarian cortical tissue culture

In the cultured groups, the fragments (N = 26 fragments in each group) were cultured individually in 96-well V-bottom culture plates for 8 days [47,48]in 300 μl α-MEM medium (Biowest, Farnce) supplemented with 10% fetal bovine serum (FBS) (Gibco, UK), 50 mg/ml streptomycin, 60 IU/ml penicillin, 10 μg/ml insulin transferrin selenium (ITS) (Gibco, UK), and 0.5 IU/ml human recombinant follicle stimulating hormone (rFSH) (Merck, Germany) at 37 °C in a humidified incubator with 5% CO_2 [49]. Two-thirds of the media was replaced with fresh media every 48 h. Aspirated media of eight fragments were stored at −20 ° C for glucose uptake and estradiol production evaluation. After the 8-day culture period, 6 fragments were immersed in RNA lather (Yekta Tajhiz Azma, Iran) for real time PCR assessments, 10 fragments were stored at −80 °C for biochemical assays, and 10 fragments were fixed for histological assessments. In addition to the cultured groups, the procedure was applied to the fragments that were not cultured for comparison.

2.5. Histological and immunohistochemical analyses

2.5.1. Histological assessment

Ten fragments from each experimental group were fixed at room temperature for 22 h using 10% formaldehyde in 0.01 M phosphate buffered saline (PBS). The samples were dehydrated, cleared, embedded in paraffin, and sectioned using a microtome (Leitz 1512, Germany) to obtain 5 μm thickness tissue section. Every tenth section was mounted on a glass slide and stained with hematoxylin and eosin [50].

The stained sections were evaluated using a 40X objective to count the follicles at different developmental stages (due to avoid of recounting the follicles, only follicle with oocyte contain nucleus were counted). The follicles were counted in 4 sections of 5 fragments in every group (totally 20 sections in each group). Follicles were considered normal when showing a round oocyte with surrounding granulosa cells in the periphery. Normal stromal cells were recognized via the fusiform nucleus. The follicles were identified based on the characteristics as follows [51]; i) Primordial follicle: containing a single layer of flattened granulosa cells, ii) Primary follicle: containing a single layer of cuboidal granulosa cells, and iii) Secondary follicle: containing two or more layers of granulosa cells.

2.5.2. Prussian blue staining

To evaluate tissue penetration of IONP@Si@PEG, prussian blue staining was utilized. 4 sections with 100 μm intervals (to evaluate surface and deep part of tissue) were mounted. Therefore, 10% potassium ferrocyanide (Sigma-Aldrich, USA) and 20% hydrochloric acid were dissolved in distilled water a 1:1 final solution was prepared. Then, the hydrated tissue sections were immediately immersed in the solution. After 20 min of incubation at room temperature, glass slides were rinsed and counterstained with nuclear fast red (Sigma-Aldrich, USA) for 5 min. Stained slides were washed with distilled water, dehydrated in 70% ethanol (twice), 90% ethanol, and 100% ethanol, and submerged twice in clear xylene, then mounted and assessed with light microscopy. Under the microscope, the blue spots were detected as iron, and pink spots were detected as cellular nuclei [52].

2.5.3. Apoptosis

From each group, 10 pairs of serial sections were selected using randomized systematic sampling and then mounted on poly-L-lysine coated slides. To indicate apoptotic cells, Terminal deoxynucleotidyl transferase dUTP nick end labeling (TUNEL) Kit (Roche, Germany) was used. The mounted sections were deparaffinized with xylene, rehydrated through descending concentrations of ethanol and rinsed for 10 min in 0.1 M PBS. In the next step, the sections were incubated with 20 μg/ml proteinase K for 20 min at room temperature. The specimens were treated with 3% H_2O_2 in methanol for 10 min to block endogenous peroxidase activity. After washing with PBS for 3 min, the specimens were incubated with the TUNEL reaction solution containing terminal deoxynucleotidyl transferase (TdT) and deoxynucleotide at 4 °C overnight. After incubation, all the sections were rinsed with PBS and conjugated with horse-radish peroxidase (POD, 1:500) for 30 min at room temperature. Then, sections were washed extensively with PBS for 3 min and treated with DAB solution (30 mg of DAB and 200 μl of H_2O_2/100 ml PBS) for 15 min at room temperature in dark. After being rinsed with tap water, all the sections were counterstained with hematoxylin for 1 min [53].

The apoptotic cells were counted by means of counting frame and stereological methods. The estimation of TUNEL-positive cells per unit area was done using a protocol provided by Ref. [54] via formula 1; Formula 1: apoptotic cells counting

$$N_A = \frac{\sum \bar{Q}}{a/f . \sum p}$$

where, N_A is the number of apoptotic cells per unit area, $\sum \bar{Q}$ is the total number of cells counted, a/f is the area of every frame counted, and $\sum p$ is the total number of frames that have been in collision with the section.

2.6. Biochemical assays

Ten fragments in each group were mechanically homogenized in cold PBS (pH = 7) and then used for all biochemical assessments. For tissue homogenization, we used Omni Tissue Homogenizer (TH) and the machine speed was 5000 rpm. Since the buffer of all three tests was PBS, each homogenized solution was used for all biochemical tests. All biochemical assessments were performed twice.

2.6.1. Malondialdehyde (MDA) level measurement

MDA is a substance produced in response to oxidative stress and damage to cell lipid membranes, therefore, MDA level is an index used to evaluate lipid peroxidation injury. MDA reacts with thiobarbituric acid (TBA) (Merck, Germany) as a TBA reactive substance (TBARS) and produces a red complex. Briefly, the samples were homogenized and 2 mL of a solution containing TBA, trichloroacetic acid, and hydrochloric acid was added. The solution was boiled in a water bath for 40 min. After cooling to room temperature, the solution was centrifuged at 1000 g for 10 min. The absorbance was read at 535 nm by a microplate reader (Epoch, BioTek, US). The MDA concentration (C) was calculated according to formula 2 [55].

Formula 2: MDA concentration measurement

$$C = \text{Absorbance}/1.56 \times 10^5$$

2.6.2. Superoxide dismutase (SOD) activity measurement

The SOD is an enzyme that facilitates the conversion of superoxide radicals (O_2^-) to O_2 or H_2O_2, therefore, it is an antioxidative agent. SOD activity was measured by a procedure described by Madesh and Balasubramanian [55]. A colorimetric assay based on generation of superoxide by pyrogallol (Merck, Germany) auto-oxidation was applied to measure inhibition of superoxide-dependent reduction of 3-(4,5-dimethylthiazol-2-yl) 2,5-diphenyltetrazolium bromide (MTT) (Sigma, USA) dye to formazan at 570 nm. One unit of SOD activity is defined as the amount of enzyme causing 50% inhibition in the MTT reduction rate.

2.6.3. Catalase (CAT) activity measurement

CAT is a strong antioxidant, and it is an enzyme that converts H_2O_2 to H_2O and O_2. CAT activity was measured according to the Aebi method with some modifications [56]. The aim of this assay is to determine the rate of hydrogen peroxide decomposition. Reduction in absorbance (at 240 nm) per minute was determined by UV–Vis spectrophotometer (Cecil, UK) and the rate of the enzyme activity was calculated.

2.7. Tissue viability by glucose uptake assay

Media from 8 fragments from cultured groups (8 wells/group) were collected for glucose uptake viability assay (glucose uptake per mg tissue per hour). The assay was used with some modifications to reflect stromal cell viability in the ovarian cortex, according to Gerritse et al. [57]. Glucose concentrations in the culture medium (between 2-4 and 6–8 days) were measured by Glucose assay kit (Pars Tous Azmon, Iran). At the end of the culture, all fragments were weighted (mg) and the amount of consumed glucose (micro-moles/mg for tissue/hour) was calculated.

2.8. Hormonal measurement

To evaluate the ovarian endocrine function, the concentration of E2 within the medium of cultured fragments (8 fragments per every cultured group) were measured at days 0, 4 and 8 of the culture. The levels of E2 were measured by an assay kit (Roche, Germany) and electrochemiluminescence (ECL). For day 0 measurements, culture medium without rFSH was collected approximately 4 h after tissue warming and incubation [58].

2.9. Molecular assessment

2.9.1. RNA extraction and cDNA synthesis

At least 6 fragments from each group were used for the molecular assessment. Total RNA was extracted from each fragment using RNA extraction kit (Pars Tous Azmon, Iran). To evaluate the integrity of extracted RNA we used agarose gel electrophoresis. The quantity and quality of extracted RNA were evaluated with Nano-drop spectrophotometer (Thermo Fisher Scientific, USA), to determine the integrity of extracted RNA we used by Agarose gel Electrophoresis, if 18S and 28S band were observed and OD 260/280 ratio more than 1.8 (mostly were near to 1.9) we used that RNA to cDNA synthesize.

The cDNA was then synthesized based on kit protocol (Pars Tous Azmon, Iran), to confirm the synthetization of cDNA we done PCR process for housekeeping gene (*GAPDH*) and assessed it with the agarose gel electrophoresis.

2.9.2. Real-time PCR

Designed primers by Gen Bank (www.ncbi.nlm.nih.gov) and oligo7 software (Table 1) were ordered (Pishgam, Iran). GAPDH was used as a housekeeping gene and internal control. 1 μl of cDNA, 2 μl of the mixture of forward and reverse primers, and 10 μl of SYBR

Green Master Mix (Ampliqon, Denmark) were mixed with pure water to reach a volume of 20 μl. After completing the real-time PCR, melt curve analysis was applied to confirm the amplified product and record the Cq (Quantification cycles) values. Finally, gene expression was calculated using the REST software (2009). All molecular evaluations were at least twice verified.

2.10. Statistical analysis

All data were analyzed using the GraphPad Prism software (version 8.0; GraphPad Software, San Diego, CA). One-way ANOVA with Bonferroni post hoc and Student's t-test (unpaired) were applied for multiple comparisons of groups and two groups, respectively. Statistical significance was established at $p < 0.05$.

3. Result

3.1. Histological evaluation

The images of histological assessments of the ovarian cortical sections are shown in Fig. 2. Based on H&E assessments after cryopreservation and warming or nanowarming process, the follicular and stromal tissue integrityin the Convl-Vit and Nano-Vit were similar to Fresh. In the AMF group, small detachments were observed between the oocyte and granulosa cells. No antral follicles were observed. After culture time the follicular and stromal tissue integrity in the Convl-Vit/Culture and Nano-Vit/Culture were less than Fresh and in AMF/Culture group were decreased in compare to other culture groups. The follicles in different stage of development were counted and presented below.

3.2. Follicular development

In total, 20 sections from each group were evaluated to assess follicular number and developmental stage in Non-Cultured groups (Fig. 3). The total normal follicles in AMF group decreased in compare to Fresh and nano-Vit (Fig. 3a). The degenerated follicles in Convl-Vit significantly increased compare to Fresh ($p < 0.01$) (Fig. 3b). Primary follicles in the non-cultured AMF group were also lower compared to the non-cultured Fresh group ($p < 0.05$) (Fig. 3d). There was no significant difference between Fresh and Nano-Vit groups. There were no significant differences in number of secondary follicles between all groups before and after culture (Figs. 3e and 4e).

Although the number of primordial follicles in all groups were initially similar (Fig. 3c), they were decreased throughout culturing period (Fig. 4c). The total normal follicles in AMF/Culture group decreased in compare to Fresh/Culture and nano-Vit/Culture (Fig. 4a) and degenerated follicles increased, too (Fig. 4b). The number of degenerated follicles in Convl-Vit/Culture was more than Fresh/Culture ($p < 0.01$) (Fig. 4b). The number of primary follicles in the AMF/Culture group was significantly lower than this number in Nano-Vit/Culture as well as in Fresh/Culture groups ($p < 0.05$) (Fig. 4d). Furthermore, Nano-Vit/Culture and Convl-Vit/Culture groups showed similar quantities of follicles in all the developmental stages that were evaluated. No significant difference was found when counting secondary follicles between all groups.

3.3. IONP penetration

Prussian blue staining showed that IONP uniformly penetrated all parts of the tissue (Fig. 5).

3.4. Oxidative stress assessments

Assessment of MDA levels are illustrated in Fig. 6a and d. The results indicate an overall increase in MDA levels where it is significant between Fresh and AMF groups. In contrast, tissues treated with Convl-Vit technique and cultured (Convl-Vit/Culture) showed a higher MDA level compared to Nano-Vit/Culture ($p < 0.05$). There was no significant difference in SOD activity of Nano-Vit and Fresh, but for AMF group, this activity seemed significantly diminished when compared to Fresh, and decreased in Convl-Vit group compared to Nano-Vit (Fig. 6b) ($p < 0.05$). Difference in SOD activity between cultured groups were not significant (Fig. 6e). There was no significant difference in CAT activity of Nano-Vit and Fresh, but this activity in AMF significantly decreased compared to the

Table 1
Specifications of primers.

Primer			Product size	TM
BMP15	Forward	GGGTTCTACGACTCCGCTTC	273	60
	Reverse	GGTTACTTTCAGGCCCATCAT		
GDF9	Forward	TAGTCAGCTGAAGTGGGACA	224	62
	Reverse	AGCCATCAGGCTCGATGGCC		
FSHR	Forward	TCTTTGCTTTTGCAGTTGCC	126	58
	Reverse	GCACAAGGAGGGACATAACATAG		
GAPDH	Forward	CTGCTGACGCTCCCATGTTTGT	150	62
	Reverse	TAAGTCCCTCCACGATGCCAAA		

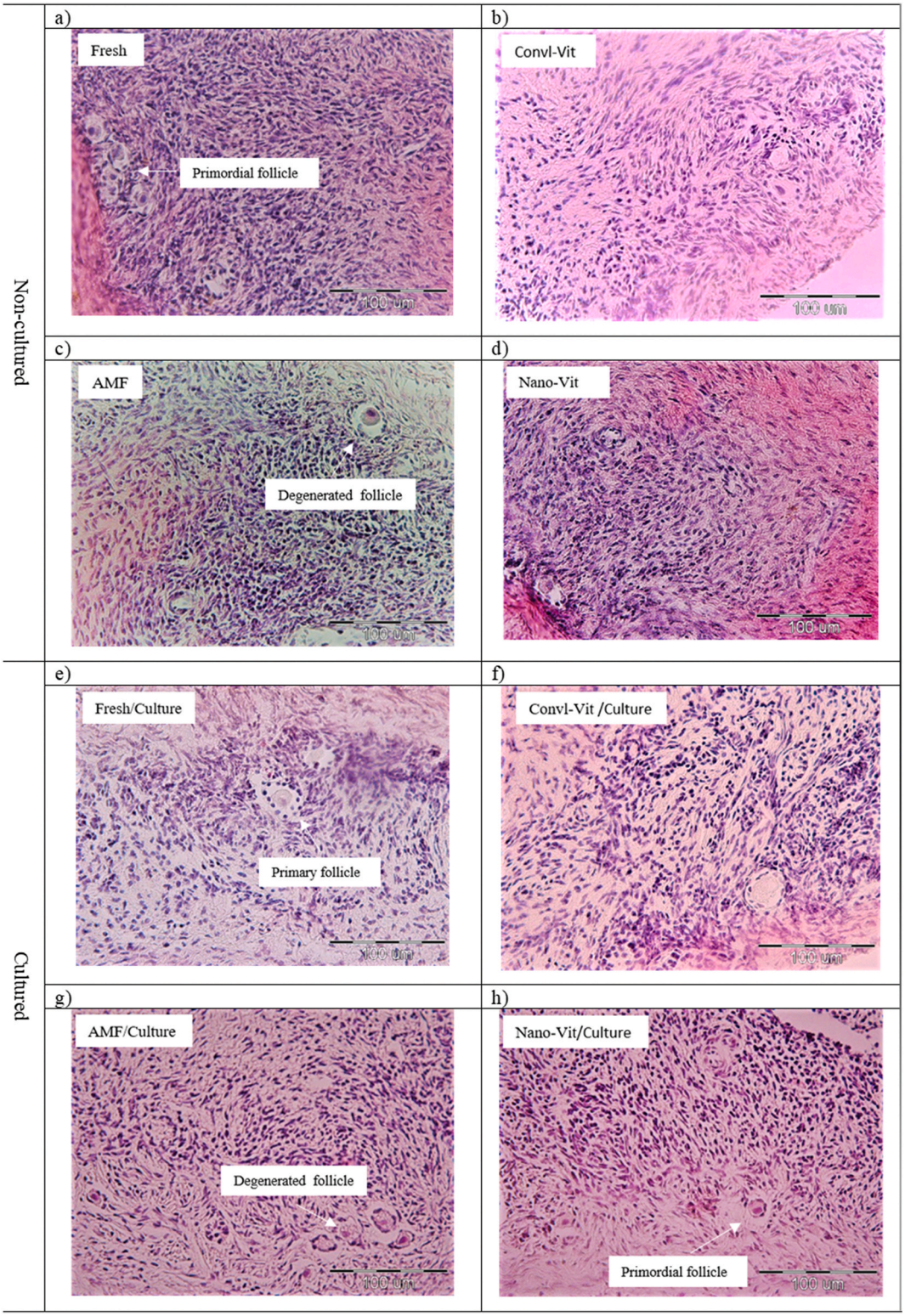

Fig. 2. Photomicrograph of cultured and non-cultured ovarian cortical tissue sections stained with Hematoxylin and eosin (H&E), (Magnification at 40X).

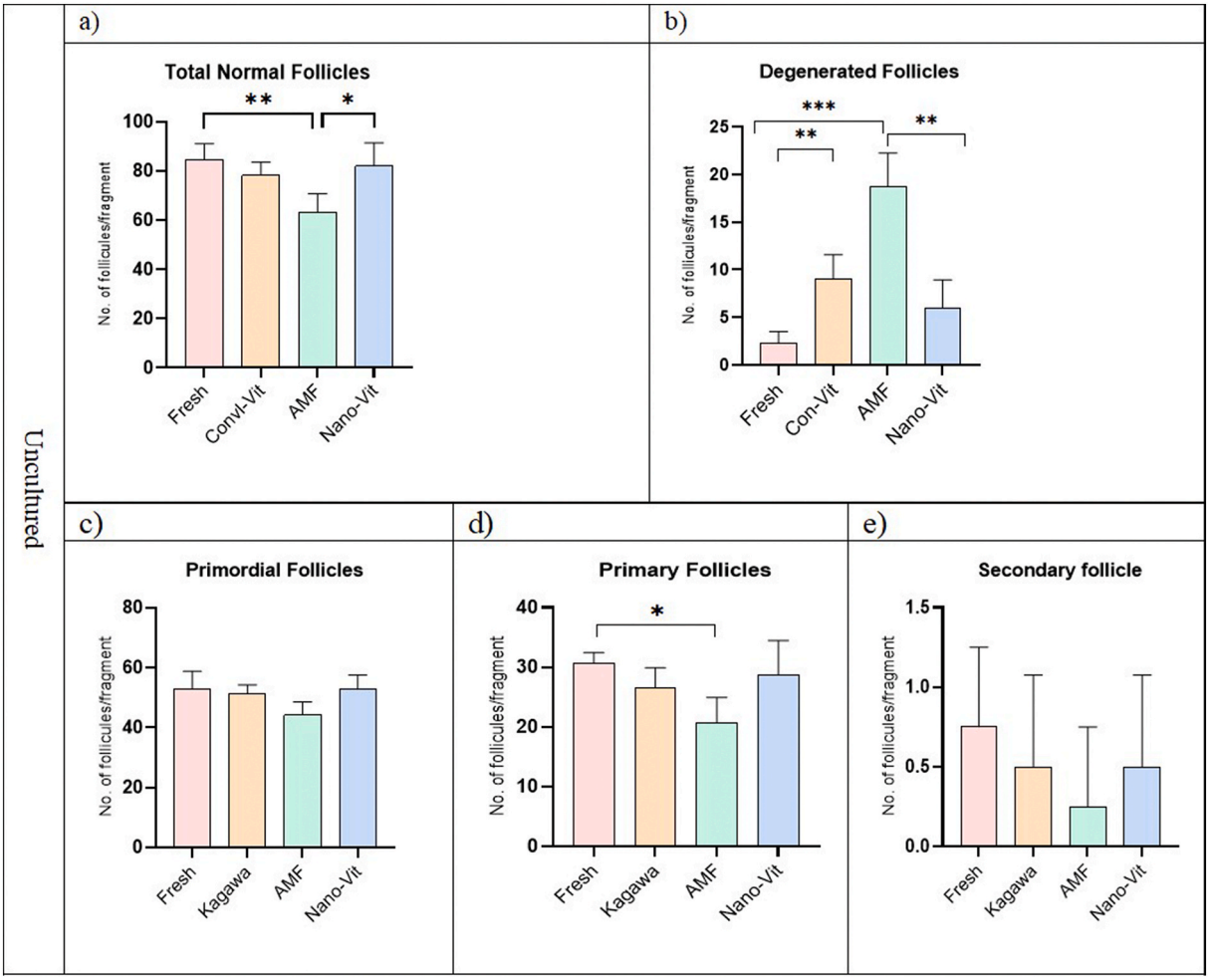

Fig. 3. The number of follicles in different developmental levels for non-cultured ovarian cortical fragments, (* indicate $p < 0.05$ and *** indicate $p < 0.001$).

Fresh (Fig. 6c) ($p < 0.05$). There was no significant difference between Fresh/Culture and Nano-Vit/Culture, the CAT activity in Nano-Vit/Culture was more than Convl-Vit/Culture (Fig. 6f) ($p < 0.05$).

3.5. Apoptosis assessment

Apoptosis was evaluated with TUNEL, and the results are depicted in Fig. 7. The apoptotic cell counts per unit area for each group is quantified and presented in Fig. 7 (i and j). Results show that the number of apoptotic cells per unit area in Nano-Vit and Convl-Vit groups are similar and were not significantly different compared to the Fresh (Fig. 7i). Expectedly, all cultured groups had a significantly higher apoptotic measures compared to freshly dissected tissue that was also cultured for 8 days (Fig. 7j).

3.6. Tissue viability

Glucose uptake can reflect the level of tissue damage as well as viability. Glucose consumption (μmol/mg per tissue/hour) between days 2–4 and 6–8 (Fig. 8a) was significantly lower in the AMF/Culture group compared to all other groups ($p < 0.001$).

3.7. Tissue function assessment

Production of steroid is a prominent function of ovaries. Secreted estradiol hormone was therefore measured in media of cultured tissues at day 0, 4 and 8 (Fig. 8b). While at day 0 there was no significant difference, at day 4, estradiol production in the Fresh/Culture group was higher than in all other groups. At day 8, the level of estradiol production increased in all groups, and in AMF/Culture group was lower than other groups. No significant difference was detected between Fresh/Culture, Nano-Vit/Culture and Convl-Vit/Culture.

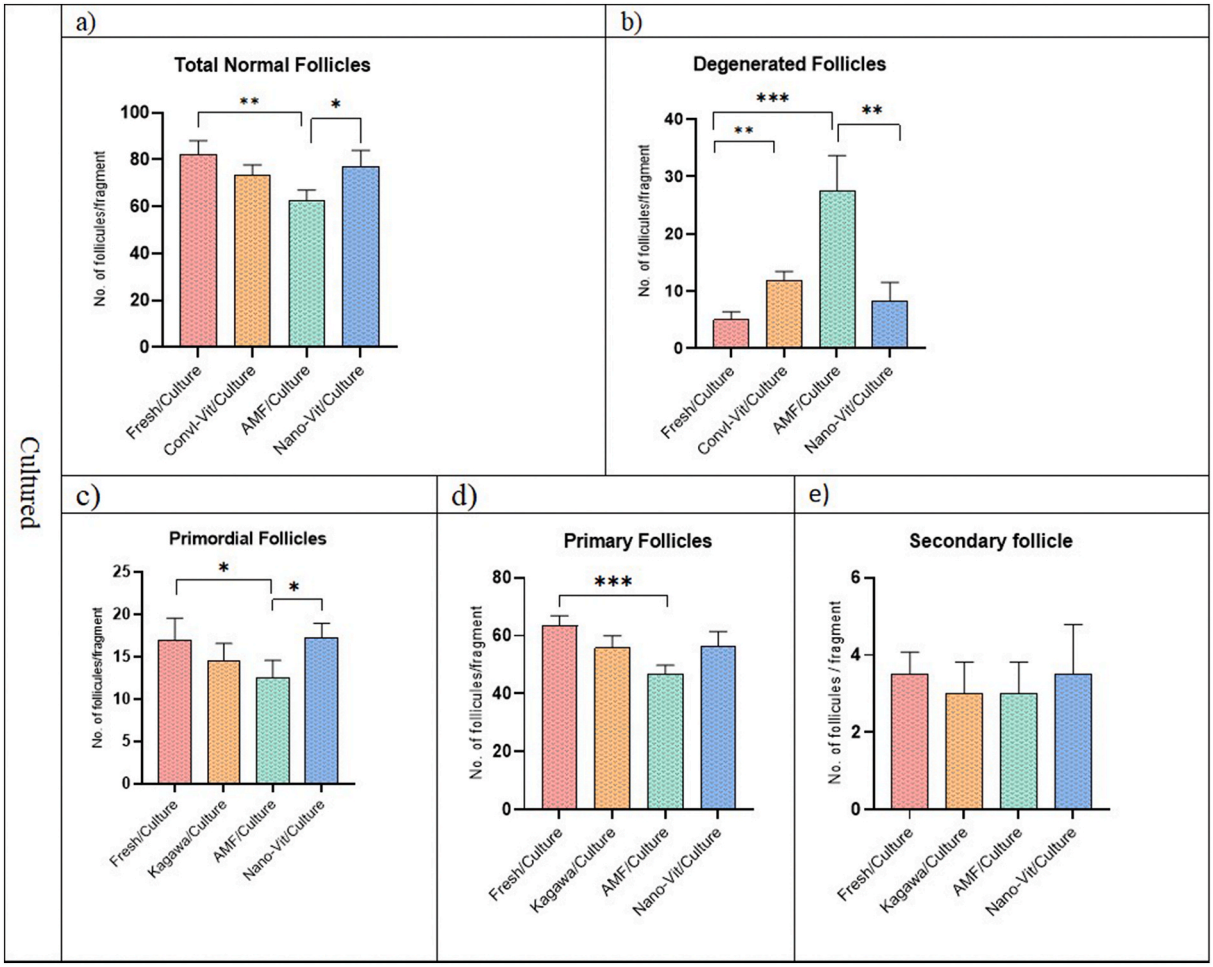

Fig. 4. The number of follicles in different developmental levels for cultured ovarian cortical fragments, (* indicate $p < 0.05$, ** indicate $p < 0.01$ and *** indicate $p < 0.001$).

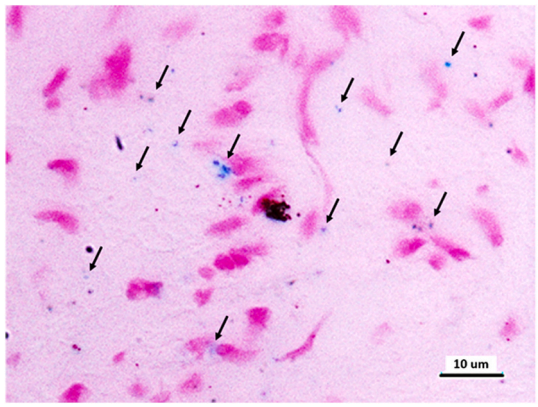

Fig. 5. Prussian blue staining of naowarming groups, that shows IONP uniformly penetrated in ovarian cortical fragments, the pink spots indicate cell nuclei and the blue spots are IONP, some of IONP are shown using arrows (Magnification of 100X).

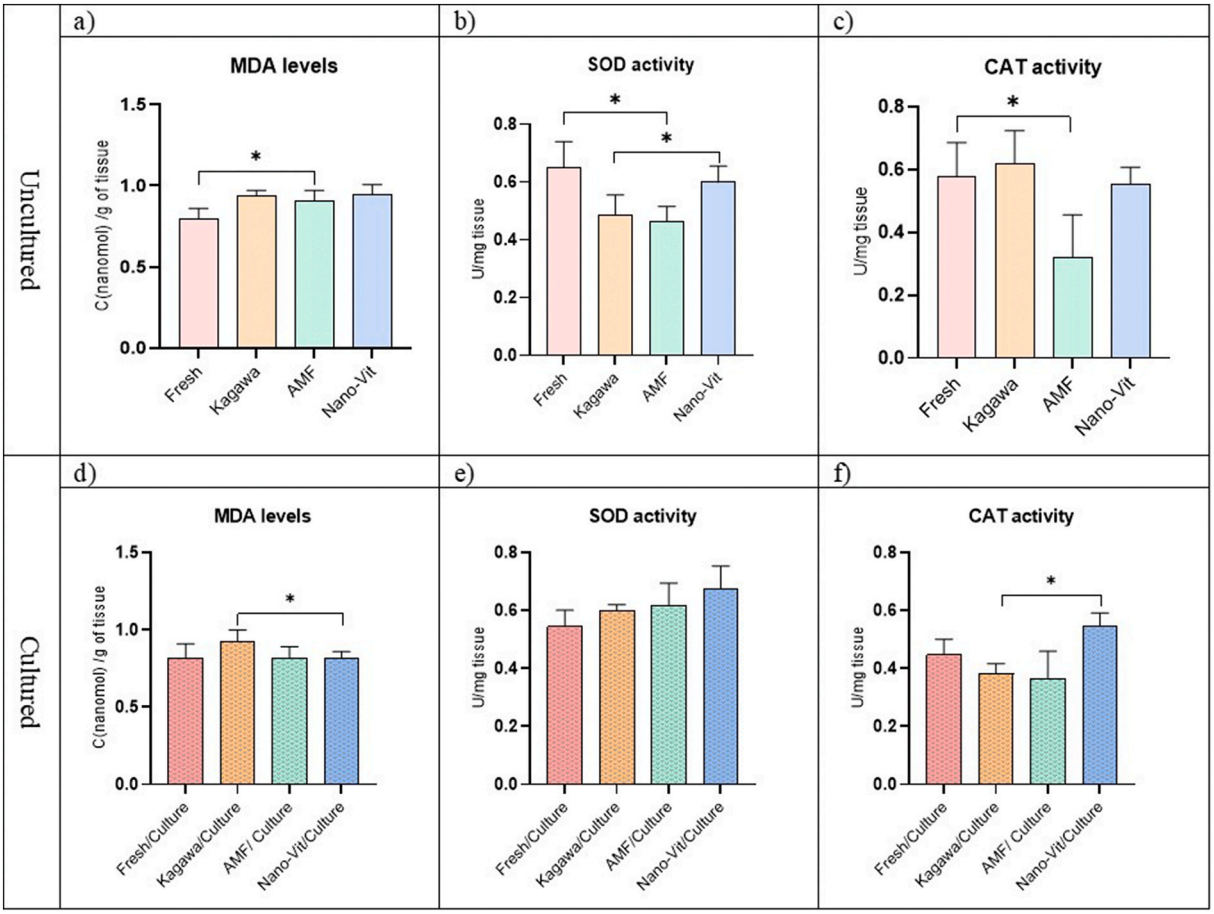

Fig. 6. Oxidative stress diagrams of all groups. (a and d) MDA levels (C: concentration), (b and e) SOD activity (U: Unit), and (c and f) CAT activity (U: Unit), (* indicates $p < 0.05$, ** indicates $p < 0.01$).

3.8. Gene expressions

Expression of folliculogenesis-related genes in all groups were analyzed. According to the results in Fig. 9a, there was no significant difference in *BMP15* expression before culture among groups. The *BMP15* in Convl-Vit/Culture was expressed lower than Nano-Vit/Culture group ($p < 0.01$) (Fig. 9d). There was no significant difference in the *GDF9* expression levels before culture (Fig. 9b), whereas after culture (Fig. 9e), the expression of *GDF9* in the AMF/Culture was significantly lower than all other groups ($p < 0.01$, $p < 0.001$). After Fresh/Culture, *GDF9* was highly expressed in Nano-Vit/Culture. The expression of *FSHR* in AMF was significantly higher than Fresh (Fig. 9c). This expression was significantly lower in cultured AMF compared to Fresh. The expression of *FSHR* in cultured Nano-Vit was higher than cultured Convl-Vit (Fig. 9f).

4. Discussion

Cryopreservation is a critical and relatively simple technique that is used to store living biological samples at very low temperatures [59]. Cryopreservation of reproductive cells and tissues is among necessary avenues to preserve fertility in patients [60]. Fertility preservation strategies vary, and they are recommended based on patient's health conditions, nevertheless, ovarian tissue vitrification is one of the important methods for fertility preservation. In 2009 a vitrification procedure by Kagawa et al. [20] was introduced that became widely accepted by the scientific community in this field [61,62]. While there are claims that ovarian cortex vitrification by conventional vitrification lacks adverse side effects [63], there are evidence that suggests otherwise [61]. More specifically, during the warming process of the cryopreserved tissue, lack of uniform and fast thermal distribution results in formation of ice particles that later leads to tissue damage [9,12]. In line with this, herein Nanowarming has been proposed as a complementary addition to conventional vitrification (Nano-Vit) to preserve live follicular counts and healthy development in cryopreserved ovaries. According to the results (Fig. 2a), there was no significant difference in the number of primordial follicles between Non-Cultured groups, so the ovarian reserve uniformity of the tissues in the start of study was approved [64]. Tissue culture is one of the methods to investigate the long-term effects of cryopreservation [65] and primordial follicles activation and maturation [66]. In the AMF group we did not use

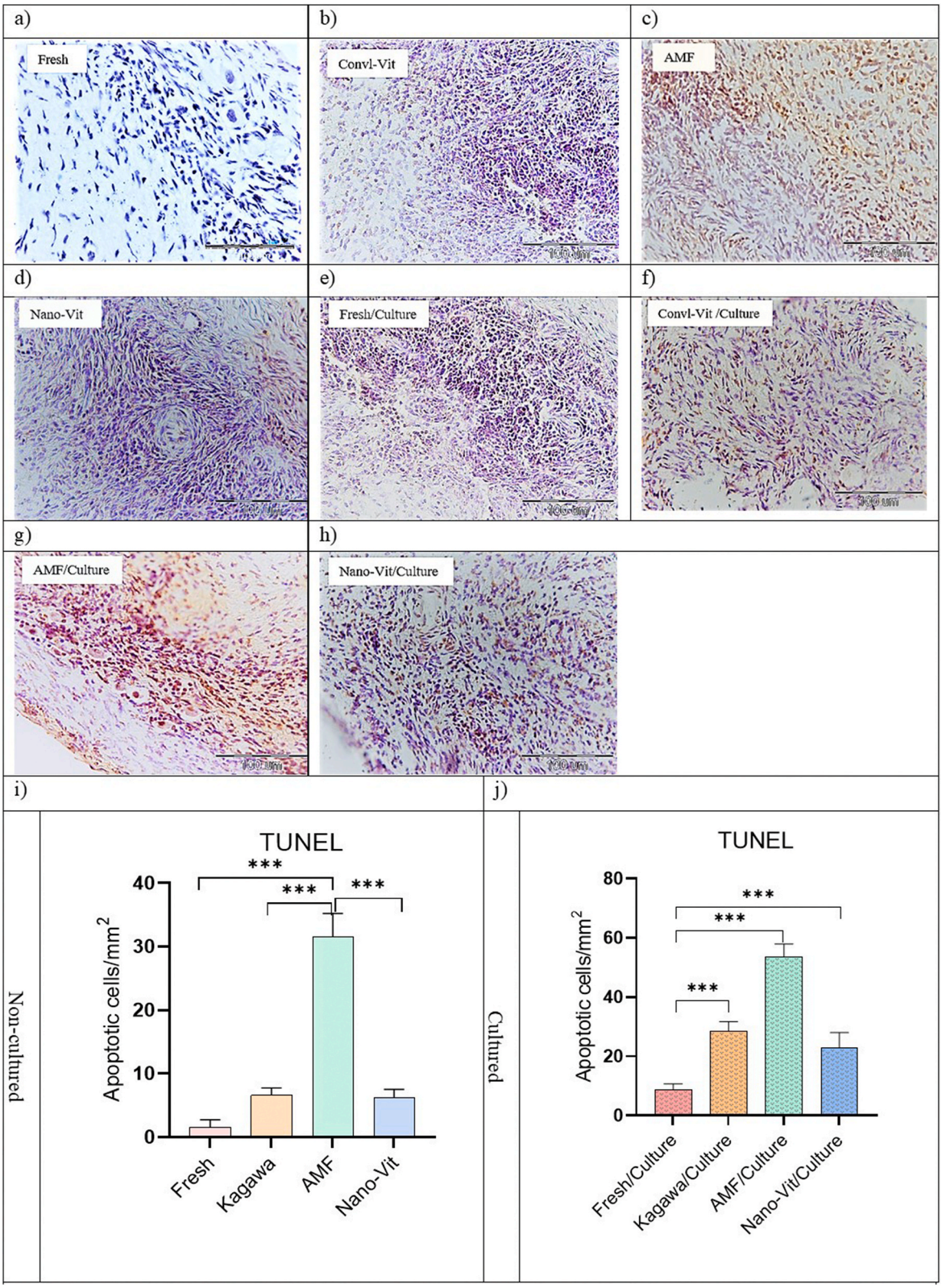

Fig. 7. a–h: Photomicrograph of cultured and non-cultured ovarian cortical tissue sections prepared with TUNEL to detect apoptotic cells. The blue nuclei are TUNEL negatives, and the brown nuclei are TUNEL positive cells (Magnification of 40X). i and j: The mean number of TUNEL positive cells per unite area in all studied groups. i) before culture, j) after culture (*** indicates $p < 0.001$).

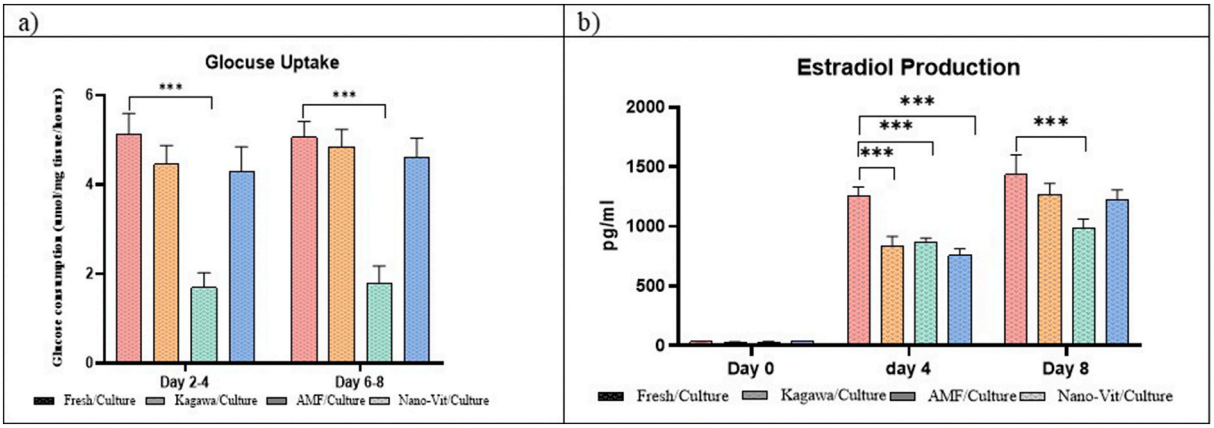

Fig. 8. a) Glucose uptake by cortical fragments b) Estradiol hormone production by ovarian cortical fragments before and after cryopreservation and warming per milligram tissue per hour of culture (* indicates $p < 0.05$, ** indicates $p < 0.01$ and *** indicates $p < 0.001$).

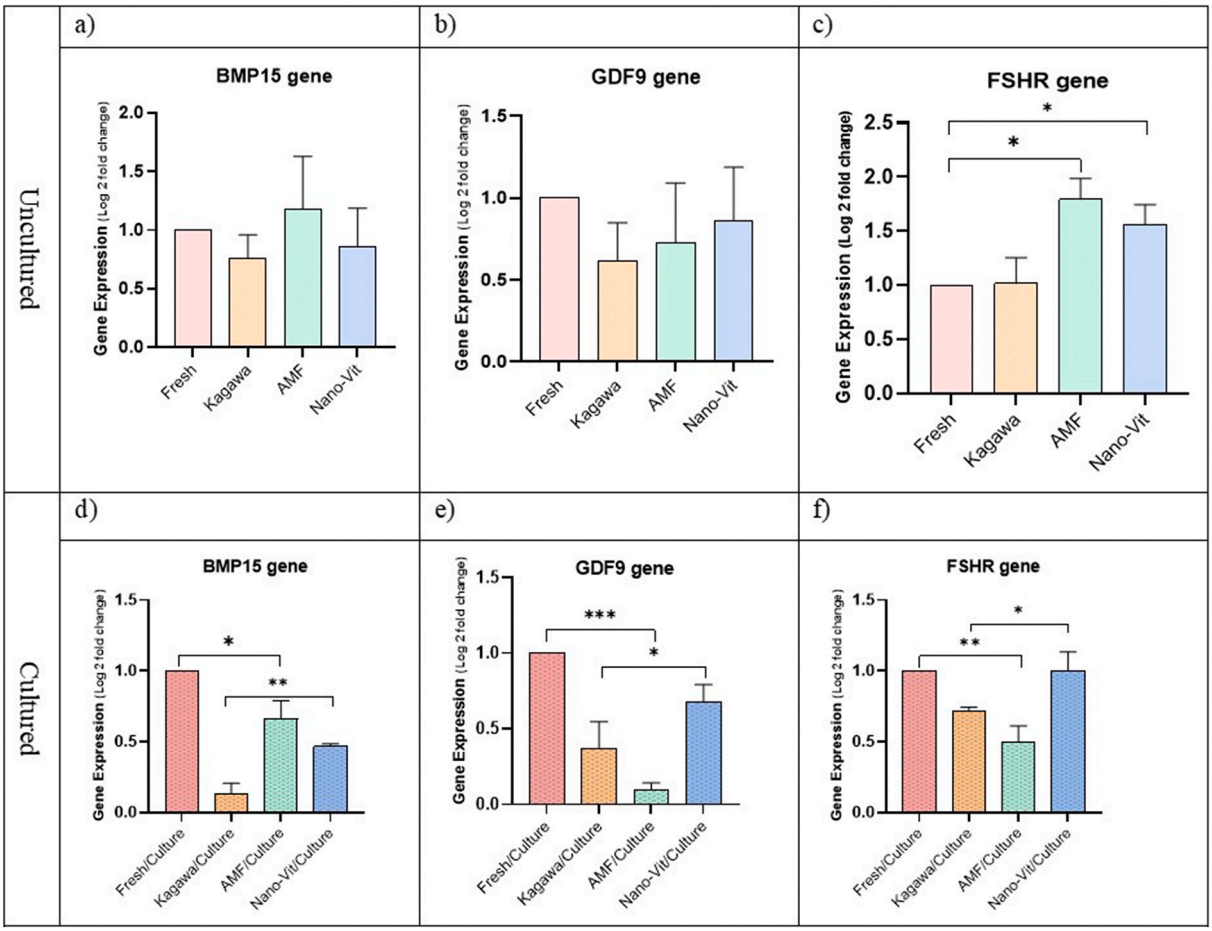

Fig. 9. Expression of folliculogenesis-related genes in non-uncultured and cultured ovarian cortical tissues post vitrification and warming. BMP15 gene expression (a and d), GDF9 gene expression (b and e), FSHR gene expression (c and f), (* indicates $p < 0.05$, ** indicates $p < 0.01$ and *** indicates $p < 0.001$).

nanoparticles in vitrification process, but we warmed the tissue inside the alternative magnetic field (just for investigation the AMF). The number of total normal follicles (Figs. 3 and 4) in AMF group were less than Fresh (Cultured and Non-Cultured), so the AMF alone did not have the ability to warm the tissue without thermomechanical damages [67]. There were no significant differences between

Nano-Vit/Culture and Fresh/Culture in follicle counted (Figs. 3 and 4), it was more than Convl-Vit/Culture but not significant (Figs. 3 and 4). Convl-Vit increased the number of degenerated follicles compare to Fresh (Cultured and Non-Cultured) (Figs. 3b and 4b). Based on Fig. 5, nanoparticles penetrate and distribute uniformly in the tissue, we concluded that Nanowarming is a technique that utilizes hyperthermia of magnetic nanoparticles to homogenously accelerate warming process.

Oxidative stress is a major contributing factor in cryoinjury [14,68] specially after human ovarian tissue cryopreservation [69,70]. The first antioxidant defense line that plays key and fundamental role in survival of biological systems is measured by levels of Malondialdehyde MDA, as well as activities of superoxide dismutase SOD and CAT. MDA is a colorless and highly reactive organic compound, and it is a marker for oxidative stress. Increased levels of MDA production is rooted in disruption of cellular bi-phospholipid membrane [15] which can be attributed by formation of ice crystals in cryoinjured tissue [14,71]. In fact, compared to the freshly dissected ovarian tissue (Fresh), MDA levels marked slightly higher mean values when cryopreserved and warmed (Fig. 6a). However, tissue fragments cultured and treated by Nano-Vit expressed significantly lower levels of MDA when compared to cultured fragments that were treated by the conventional vitrification technique (Fig. 6d). SOD is an enzyme that catalyzes the dismutation of the superoxide radicals, a by-product of oxygen metabolism, into ordinary molecular oxygen and hydrogen peroxide which undergoes degradation by CAT [72]. SOD acts as a therapeutic agent against reactive oxygen species-mediated diseases [72] and, if not regulated, causes many types of cell damage [73]. Results in Fig. 6b show that Nano-Vit had no significant impact on SOD activity, but conventional vitrification exhibits a significantly lower SOD. In other words, there are similar levels of enzyme activity between ovarian tissue fragments that are cryopreserved and rewarmed by Nano-Vit and freshly dissected ovarian tissues. CAT, an enzyme that catalyzes the reaction by which hydrogen peroxide is decomposed to water and oxygen [72], also plays an important role in regulating oxidative stress. Fig. 7c shows that both Convl-Vit and Nano-Vit display similar levels of CAT activity. However, when cultured, Nano-Vit shows higher levels of CAT activity with respect to Convl-Vit (Fig. 6f). This indicates that ultimately, Nano-Vit constitutes lower levels of oxidative stress than the Convl-Vit. This is despite confounding evidence that iron nanoparticles can contribute to oxidative stress [74,75]. However, it is arguably hypothesized that the silica coating as well as PEGylation of IONP used in Nano-Vit procedure constitute a preventive shield against induction of this stress [44].

Apart from oxidative stress, cryopreservation can also induce some levels of cellular apoptosis [76]. Some researches indicated different level of apoptosis after vitrification in human ovarian tissue [77], that it accrues after cryopreservation with different methods, such as slow freezing, open and close vitrification [38], using optimized and modified method for cryopreservation decreased the apoptosis [78]. However, Shore et al. [79] showed that when coupled with Nanowarming, vitrified human dermal fibroblast cells express elevated levels of viability post warming process. Another study indicated that vitrification and Nanowarming of porcine aortic heart valve tissue decreased the number of TUNEL positive cells and enhanced the cell viability compared to the conventional warming method [80]. In this study, TUNEL assessments (Fig. 7) illustrated that the occurrence of cellular apoptosis for Convl-Vit and Nano-Vit were very similar to that of freshly dissected tissue (Fig. 7i). Expectedly, cryopreserved tissue fragments that are warmed (via Nano-Vit or Convl-Vit techniques) and cultured are highly expressive of apoptotic cells (Fig. 7j).

Glucose uptake from culture medium is a reliable assessment of tissue viability [57]. Fig. 8a suggests that glucose uptake levels did not significantly vary between Fresh/Culture, Convl-Vit/Culture, and Nano-Vit/Culture. Estradiol secretion by granulosa cells under FSH stimulation is another reliable indicator of secondary follicle transition to antral follicle [81–83] and therefore a marker of tissue viability. According to Fig. 8b, Convl-Vit/Culture and Nano-Vit/Culture produced lower levels of estradiol than Fresh/Culture on the fourth day of culture, they seem to have caught up with estradiol secretion levels of Fresh/Culture on day eight. This finding is in agreement with another study that suggests low estradiol secretion levels on the fourth day of culture can be compensated if vitrified-warmed tissue is kept in culture for eight days [58,84].

Another indicator of follicular development is gene expression levels of *BMP15* and *GDF9* in oocytes, immature eggs, that dictates the developmental transformation of primary to secondary follicles [17,85]. In addition, expression levels of *FSHR* in granulosa cells as an indicator of healthy transition from secondary follicles to antral follicles [18] were examined. While *BMP15* and *GDF9* expression levels were similar among all non-cultured groups (Fig. 9), these expression levels for cultured fragments that were treated by Nano-Vit (Nano-Vit/Culture) were significantly higher than Convl-Vit/Culture and closer to gene expression levels of Fresh/Culture (Fig. 9d). With respect to *FSHR*, Convl-Vit showed a better expression in non-cultured samples (Fig. 9c), but with respect to cultured samples, Nano-Vit/Culture excelled (Fig. 9f).

The results in this study indicate that with respect to follicular count, follicular development, oxidative stress, tissue viability, and expression of follicular developmental genes, there are no significant difference between cultured ovarian fragments undergone Nano-Vit procedure (Nano-Vit/Culture) and freshly dissected and cultured tissue (Fresh/Culture). Therefore, Nanowarming protected the ovarian tissue from injury during vitrification and warming process. While Nanowarming can be suitably applied to large tissue samples [31,80], the current feasibility study aimed at providing sufficient evidence that the approach is sound. Generally, the results presented in this investigation have shown a potential for Nano-Vit to become a complementary addition to the conventional vitrification technique. Vitrified ovarian tissues are often warmed and cultured or transplanted [86]. This allows for the revival of some of the lost tissue functions due to vitrification before it is placed back in the body. Evidently, Nano-Vit/Culture bested in this setting. Nevertheless, there need to be many important assessments before the proposed technique becomes a viable solution in fertility. This study faced to some limitation, because of culture process and the nutrition of tissue we had to section the fragments in small size. Arguably, finding ways to vitrify without having to slice the ovarian tissue into small fragments can allow a better assessment of the techniques. Also, it is important to assess the short- and long-term effects of coated IONP in the rewarmed and transplanted ovarian tissue as well as its downstream consequences on fertilization and potential embryos. We studied on sheep ovary as human model for the first step, but for more advance studies we suggest utilize exceed human ovarian tissue (after therapeutic surgeries) and xenograft on animal after cryopreservation and nanowarming process. Xenograft allows the use of larger tissue fragments for cryopreservation

and nanowarming and in-vivo evaluation of ovarian tissue function. In addition, due to the lack of access to some equipment, we could not record the process of uniform diffusion of heat in the tissue, for more studies we propose more evaluation in this line, too.

5. Conclusion

Cryopreservation, as a beneficial technology for long-term storage of biomaterials, faces technical challenges, especially during thawing process. Nanowarming by hyperthermia of PEGylated silica-coated magnetic nanoparticles has presented a new avenue to help limit cryoinjuries. Our findings suggest that cryopreserved ovarian fragments undergone Nanowarming experience substantially lower levels of oxidative stress and some of their most important gene expressions (BMP15, GDF9 and FSHR) are kept in balance after culture. The result of this investigation concludes that Nanowarming of cryopreserved ovarian tissue has the potential to protect the tissue from cryoinjury.

Funding

This work is supported by School of Medicine, Mashhad University of Medical Sciences, Mashhad, Iran (MUMS) and the Shahid Beheshti University of Medical Sciences, Tehran, Iran (SBMU). The study was funded by Mashhad University of Medical Sciences (Project No: 970832).

Ethics approval

All procedures were performed in accordance with the guidelines approved by the Shahid Beheshti University of Medical Sciences Ethics Committee (IR.SBMU.MSP.REC.1398.981).

Consent to participate

Not applicable.

Consent for publication

Not applicable.

Availability of data and material

Data are available upon request from the authors.

Code availability

Not applicable.

Author contribution

Sareh Karimi

1. Conceived and designed the experiments
2. Performed the experiments
3. Analyzed and interpreted the data
4. Wrote the paper

Seyed Nasrollah Tabatabaei

1. Conceived and designed the experiments
2. Wrote the paper
3. Contributed reagents, materials, analysis tools or data

Marefat Ghaffari Novin

1. Analyzed and interpreted the data;
2. Wrote the paper
3. Contributed reagents, materials, analysis tools or data
4. Final approval of the version submitted.

Mahsa Kazemi

1. Performed the experiments
2. Contributed reagents, materials, analysis tools or data
3. Wrote the paper.

Zahra Shams Mofarahe

1. Analyzed and interpreted the data
2. Contributed reagents, materials, analysis tools or data
3. Wrote the paper

Alireza Ebrahimzadeh-Bideskan

1. Conceived and designed the experiments
2. Analyzed and interpreted the data
3. Contributed reagents, materials, analysis tools or data
4. Wrote the paper
5. Final approval of the version submitted

Declaration of competing interest

The authors declare no competing interests.

References

[1] N. Li, et al., Predictions of mortality related to four major cancers in China, 2020 to 2030, Cancer Commun. 41 (5) (2021) 404–413.
[2] S. Lee, S. Ozkavukcu, S.-Y. Ku, Current and future perspectives for improving ovarian tissue cryopreservation and transplantation outcomes for cancer patients, Reprod. Sci. 28 (6) (2021) 1746–1758.
[3] A.Y. Ting, S.F. Mullen, M.B. Zelinski, Vitrification of ovarian tissue for fertility preservation, in: Pediatric and Adolescent Oncofertility, Springer, 2017, pp. 79–97.
[4] K. Oktay, et al., Fertility preservation in patients with cancer: ASCO clinical practice guideline update, J. Clin. Oncol. 36 (19) (2018) 1994–2001.
[5] K. Oktay, G. Karlikaya, Ovarian function after transplantation of frozen, banked autologous ovarian tissue, 1919, N. Engl. J. Med. 342 (25) (2000) 1919.
[6] F. Pacheco, K. Oktay, Current success and efficiency of autologous ovarian transplantation: a meta-analysis, Reprod. Sci. 24 (8) (2017) 1111–1120.
[7] M.M. Dolmans, T. Falcone, P. Patrizio, Importance of patient selection to analyze in vitro fertilization outcome with transplanted cryopreserved ovarian tissue, Fertil. Steril. 114 (2) (2020) 279–280.
[8] R. Lew, Natural history of ovarian function including assessment of ovarian reserve and premature ovarian failure, Best Pract. Res. Clin. Obstet. Gynaecol. 55 (2019) 2–13.
[9] G. Kim, et al., Effectiveness of slow freezing and vitrification for long-term preservation of mouse ovarian tissue, Theriogenology 75 (6) (2011) 1045–1051.
[10] M.H. Shahsavari, et al., Impacts of different synthetic polymers on vitrification of ovarian tissue, Cryobiology 94 (2020) 66–72.
[11] T. El Cury-Silva, et al., Cryoprotectant agents for ovarian tissue vitrification: systematic review, Cryobiology 103 (2021) 7–14.
[12] J. Shaw, G. Jones, Terminology associated with vitrification and other cryopreservation procedures for oocytes and embryos, Hum. Reprod. Update 9 (6) (2003) 583–605.
[13] N. Manuchehrabadi, et al., Nanowarming of tissues, Cryobiology 3 (73) (2016) 422.
[14] G. Galbiati, et al., Bilirubin, a physiological antioxidant, can improve cryopreservation of human hepatocytes, J. Pediatr. Gastroenterol. Nutr. 50 (6) (2010) 691–693.
[15] M.N. Bucak, A. Ateşşahin, A. Yüce, Effect of anti-oxidants and oxidative stress parameters on ram semen after the freeze–thawing process, Small Rumin. Res. 75 (2–3) (2008) 128–134.
[16] M. Ramezani, M. Salehnia, M. Jafarabadi, Short term culture of vitrified human ovarian cortical tissue to assess the cryopreservation outcome: molecular and morphological analysis, J. Reproduction Infertil. 18 (1) (2017) 162.
[17] F. Otsuka, K.J. McTavish, S. Shimasaki, Integral role of GDF-9 and BMP-15 in ovarian function, Mol. Reprod. Dev. 78 (1) (2011) 9–21.
[18] H. Picton, et al., The in vitro growth and maturation of follicles, Reproduction 136 (6) (2008) 703.
[19] N. Suzuki, J. Donnez, Gonadal Tissue Cryopreservation in Fertility Preservation, Springer, 2016.
[20] N. Kagawa, S. Silber, M. Kuwayama, Successful vitrification of bovine and human ovarian tissue, Reprod. Biomed. Online 18 (4) (2009) 568–577.
[21] D.P. Eisenberg, P.S. Steif, Y. Rabin, On the effects of thermal history on the development and relaxation of thermo-mechanical stress in cryopreservation, Cryogenics 64 (2014) 86–94.
[22] P.K. Solanki, J.C. Bischof, Y. Rabin, Thermo-mechanical stress analysis of cryopreservation in cryobags and the potential benefit of nanowarming, Cryobiology 76 (2017) 129–139.
[23] P.S. Steif, M.C. Palastro, Y. Rabin, The effect of temperature gradients on stress development during cryopreservation via vitrification, Cell Preserv. Technol. 5 (2) (2007) 104–115.
[24] M.L. Etheridge, et al., RF heating of magnetic nanoparticles improves the thawing of cryopreserved biomaterials, Technology 2 (3) (2014) 229–242.
[25] S. Evans, Electromagnetic rewarming: the effect of CPA concentration and radio source frequency on uniformity and efficiency of heating, Cryobiology 40 (2) (2000) 126–138.
[26] P.S. Ruggera, G.M. Fahy, Rapid and uniform electromagnetic heating of aqueous cryoprotectant solutions from cryogenic temperatures, Cryobiology 27 (5) (1990) 465–478.
[27] T. Wang, et al., Numerical simulation of the effect of superparamagnetic nanoparticles on microwave rewarming of cryopreserved tissues, Cryobiology 68 (2) (2014) 234–243.
[28] M. Schmehl, E. Graham, S. Kilkowski, Thermographic studies of phantom and canine kidneys thawed by microwave radiation, Cryobiology 27 (3) (1990) 311–318.
[29] M. Zeinoun, et al., Enhancing magnetic hyperthermia nanoparticle heating efficiency with non-sinusoidal alternating magnetic field waveforms, Nanomaterials 11 (12) (2021) 3240.

[30] Y. Bao, et al., Magnetic nanoparticles: material engineering and emerging applications in lithography and biomedicine, J. Mater. Sci. 51 (1) (2016) 513–553.
[31] N. Manuchehrabadi, et al., Improved tissue cryopreservation using inductive heating of magnetic nanoparticles, Sci. Transl. Med. 9 (379) (2017), eaah4586.
[32] F.D. Cojocaru, et al., Biopolymers–Calcium phosphates composites with inclusions of magnetic nanoparticles for bone tissue engineering, Int. J. Biol. Macromol. 125 (2019) 612–620.
[33] A. Gholami, et al., Current trends in chemical modifications of magnetic nanoparticles for targeted drug delivery in cancer chemotherapy, Drug Metab. Rev. 52 (1) (2020) 205–224.
[34] S. Sitthichai, et al., Synthesis and characterization of NiFe2O4 magnetic nanoparticles for magnetic resonance imaging application, Int. J. Nanosci. 20 (5) (2021), 2150047.
[35] D. Bobo, et al., Nanoparticle-based medicines: a review of FDA-approved materials and clinical trials to date, Pharmaceut. Res. 33 (10) (2016) 2373–2387.
[36] A. Revel, et al., Whole sheep ovary cryopreservation and transplantation, Fertil. Steril. 82 (6) (2004) 1714–1715.
[37] B.K. Campbell, et al., Ovarian autografts in sheep as a model for studying folliculogenesis, Mol. Cell. Endocrinol. 163 (1–2) (2000) 131–139.
[38] V. Padmanabhan, A. Veiga-Lopez, Sheep models of polycystic ovary syndrome phenotype, Mol. Cell. Endocrinol. 373 (1–2) (2013) 8–20.
[39] N. Kagawa, S. Silber, M. Kuwayama, Successful vitrification of bovine and human ovarian tissue, Reprod. Biomed. Online 18 (4) (2009) 568–577.
[40] J. Hao, et al., Resveratrol supports and alpha-naphthoflavone disrupts growth of human ovarian follicles in an in vitro tissue culture model, Toxicol. Appl. Pharmacol. 338 (2018) 73–82.
[41] S.H. Wu, et al., PEGylated silica nanoparticles encapsulating multiple magnetite nanocrystals for high-performance microscopic magnetic resonance angiography, J. Biomed. Mater. Res. B Appl. Biomater. 99 (1) (2011) 81–88.
[42] F.-H. Chen, et al., Synthesis of a novel magnetic drug delivery system composed of doxorubicin-conjugated Fe 3 O 4 nanoparticle cores and a PEG-functionalized porous silica shell, Chem. Commun. 46 (45) (2010) 8633–8635.
[43] G. Kalaiselvi, et al., Preparation and characterization of streptavidin-biotin aptamer coated magnetic nanoparticle for colour based detection system of antibiotic residues in biological samples, Int. J. Commun. Syst. 10 (2) (2022) 11–16.
[44] S. Karimi, et al., The effect of PEGylated iron oxide nanoparticles on sheep ovarian tissue: an ex-vivo nanosafety study, Heliyon 6 (9) (2020), e04862.
[45] T. Mazoochi, et al., Morphologic, ultrastructural, and biochemical identification of apoptosis in vitrified-warmed mouse ovarian tissue, Fertil. Steril. 90 (4 Suppl) (2008) 1480–1486.
[46] Z.S. Mofarahe, M.G. Novin, M. Salehnia, Folliculogenesis-associated genes expression in human vitrified ovarian tissue after xenotransplantation in γ-irradiated mice, Cell J. 22 (3) (2020) 350.
[47] P. Thuwanut, et al., Influence of hydrogel encapsulation during cryopreservation of ovarian tissues and impact of post-thawing in vitro culture systems in a research animal model, Clin. Exp. Reprod. Med. 48 (2) (2021) 111.
[48] Z. Ghezelayagh, et al., The effect of agar substrate on growth and development of cryopreserved-thawed human ovarian cortical follicles in organ culture, Eur. J. Obstet. Gynecol. Reprod. Biol. 258 (2021) 139–145.
[49] M. Hosseini, et al., Improvement of in situ follicular activation and early development in cryopreserved human ovarian cortical tissue by Co-culturing with mesenchymal stem cells, Cells Tissues Organs 208 (1–2) (2019) 48–58.
[50] A. Sadeghi, et al., The effect of ascorbic acid and garlic administration on lead-induced neural damage in rat offspring's hippocampus, Iran. J. Basic Med. Sci. 16 (2) (2013) 157.
[51] A.L. Kierszenbaum, L. Tres, Histology and Cell Biology: an Introduction to Pathology E-Book, Elsevier Health Sciences, 2015.
[52] H. Jouihan, Iron-Prussian blue reaction-Mallory's method, Bioprotocol 2 (13) (2012) 3–6.
[53] S.H. Rastegar-Moghaddam, et al., Maternal exposure to atrazine induces the hippocampal cell apoptosis in mice offspring and impairs their learning and spatial memory, Toxin Rev. 38 (2018) 298–306.
[54] F. Mobaraki, et al., Effects of MDMA (ecstasy) on apoptosis and heat shock protein (HSP70) expression in adult rat testis, Toxicol. Mech. Methods 28 (3) (2018) 219–229.
[55] F. Beheshti, et al., The effects of vitamin C on hypothyroidism-associated learning and memory impairment in juvenile rats, Metab. Brain Dis. 32 (3) (2017) 703–715.
[56] H. Aebi, [13] Catalase in vitro, in: Methods in Enzymology, Elsevier, 1984, pp. 121–126.
[57] R. Gerritse, et al., Glucose/lactate metabolism of cryopreserved intact bovine ovaries as a novel quantitative marker to assess tissue cryodamage, Reprod. Biomed. Online 23 (6) (2011) 755–764.
[58] L. Bastings, et al., Efficacy of ovarian tissue cryopreservation in a major European center, J. Assist. Reprod. Genet. 31 (8) (2014) 1003–1012.
[59] D.E. Pegg, Principles of cryopreservation, in: Cryopreservation and Freeze-Drying Protocols, Springer, 2007, pp. 39–57.
[60] M. Lambertini, et al., Cancer and fertility preservation: international recommendations from an expert meeting, BMC Med. 14 (1) (2016) 1.
[61] Y. Nakamura, et al., Residual ethylene glycol and dimethyl sulphoxide concentration in human ovarian tissue during warming/thawing steps following cryopreservation, Reprod. Biomed. Online 35 (3) (2017) 311–313.
[62] Q. Zhao, et al., Vitrification freezing of large ovarian tissue in the human body, J. Ovarian Res. 12 (1) (2019) 1–8.
[63] C.G. Almodin, et al., Vitrification technique for female germinative tissue cryopreservation and banking, JBRA Assist Reprod. 24 (2) (2020) 128.
[64] B.N. Cavalcante, et al., Effects of melatonin on morphology and development of primordial follicles during in vitro culture of bovine ovarian tissue, Reprod. Domest. Anim. 54 (12) (2019) 1567–1573.
[65] Z. Ghezelayagh, N. Khoshdel-Rad, B. Ebrahimi, Human ovarian tissue in-vitro culture: primordial follicle activation as a new strategy for female fertility preservation, Cytotechnology (2022) 1–15.
[66] C. De Roo, et al., In-vitro fragmentation of ovarian tissue activates primordial follicles through the Hippo pathway, Human Reprod. Open 2020 (4) (2020) hoaa048.
[67] J. Pan, et al., Investigation of electromagnetic resonance rewarming enhanced by magnetic nanoparticles for cryopreservation, Langmuir 35 (23) (2018) 7560–7570.
[68] H.K. Luz, et al., Catalase prevents lipid peroxidation and enhances survival of caprine preantral follicles cryopreserved in a 1, 2-propanediol-freezing medium, Biopreserv. Biobanking 10 (4) (2012) 338–342.
[69] B. Kim, et al., Role of klotho as a modulator of oxidative stress associated with ovarian tissue cryopreservation, Int. J. Mol. Sci. 22 (24) (2021), 13547.
[70] Z. Bahroudi, et al., Review of ovarian tissue cryopreservation techniques for fertility preservation, J. Gyn. Obs. Hum. Rep. (2021), 102290.
[71] T.H. Jang, et al., Cryopreservation and its clinical applications, Integ. Med. Res. 6 (1) (2017) 12–18.
[72] V. Baldim, et al., The enzyme-like catalytic activity of cerium oxide nanoparticles and its dependency on Ce 3+ surface area concentration, Nanoscale 10 (15) (2018) 6971–6980.
[73] F. Bellanti, et al., Many faces of mitochondrial uncoupling during age: damage or defense? J. Gerontol. Ser. A: Biomed. Sci. Med. Sci. 68 (8) (2013) 892–902.
[74] S. Mondal, et al., Hydroxyapatite coated iron oxide nanoparticles: a promising nanomaterial for magnetic hyperthermia cancer treatment, Nanomaterials 7 (12) (2017) 426.
[75] S. Abdollahii, et al., Adverse effects of some of the most widely used metal nanoparticles on the reproductive system, J. Infer. Reprod. Biol. 8 (3) (2020) 22–32.
[76] D. Zhang, et al., ROS-induced oxidative stress and apoptosis-like event directly affect the cell viability of cryopreserved embryogenic callus in Agapanthus praecox, Plant Cell Rep. 34 (9) (2015) 1499–1513.
[77] A. Dalman, et al., Slow freezing versus vitrification technique for human ovarian tissue cryopreservation: an evaluation of histological changes, WNT signaling pathway and apoptotic genes expression, Cryobiology 79 (2017) 29–36.
[78] S. Herraiz, et al., Improving ovarian tissue cryopreservation for oncologic patients: slow freezing versus vitrification, effect of different procedures and devices, e1, Fertil. Steril. 101 (3) (2014) 775–784.
[79] D. Shore, et al., Nanowarming using Au-tipped Co 35 Fe 65 ferromagnetic nanowires, Nanoscale 11 (31) (2019) 14607–14615.
[80] N. Manuchehrabadi, et al., Improved tissue cryopreservation using inductive heating of magnetic nanoparticles, Sci. Transl. Med. 9 (379) (2017).

[81] C.M. François, et al., A novel action of follicle-stimulating hormone in the ovary promotes estradiol production without inducing excessive follicular growth before puberty, Sci. Rep. 7 (2017), 46222.
[82] K.L. Britt, et al., Estrogen actions on follicle formation and early follicle development, Biol. Reprod. 71 (5) (2004) 1712–1723.
[83] S. Sanfilippo, et al., Quality and functionality of human ovarian tissue after cryopreservation using an original slow freezing procedure, J. Assist. Reprod. Genet. 30 (1) (2013) 25–34.
[84] L. Bastings, et al., Efficacy of ovarian tissue cryopreservation in a major European center, J. Assist. Reprod. Genet. 31 (8) (2014) 1003–1012.
[85] T.-r. Wang, et al., Human single follicle growth in vitro from cryopreserved ovarian tissue after slow freezing or vitrification, Hum. Reprod. 31 (4) (2016) 763–773.
[86] S. Kim, et al., Ovarian tissue cryopreservation and transplantation in patients with cancer, Obs. Gynec. Sci. 61 (4) (2018) 431–442.